Breaking Lorentz reciprocity to overcome the time-bandwidth limit in physics and engineering

K. L. Tsakmakidis[1†‡*], L. Shen[2†*], S. A. Schulz[1⊥], X. Zheng[3], J. Upham[1], X. Deng[2], H. Altug[4], A. F. Vakakis[5], and R. W. Boyd[1,6*]

[1]Department of Physics and Max Planck Centre for Extreme and Quantum Photonics, University of Ottawa, 25 Templeton Street, Ottawa, ON, K1N 6N5, Canada
[2]Institute of Space Science and Technology, Nanchang University, Nanchang 330031, China
[3]State Key Laboratory of Modern Optical Instrumentation, Zhejiang University, Hangzhou 310027, China
[4]Bioengineering Department, EPFL – École Polytechnique Fédérale de Lausanne, 1015 Lausanne, Switzerland
[5]Department of Mechanical Science and Engineering, University of Illinois at Urbana-Champaign, 1206 West Green Street, Urbana, IL 61801, USA
[6]Institute of Optics and Department of Physics and Astronomy, University of Rochester, Rochester, NY 14627, USA

†These authors contributed equally.
‡Current address: Bioengineering Department, EPFL – École Polytechnique Fédérale de Lausanne, 1015 Lausanne, Switzerland
⊥Current address: Centre for Advanced Photonics & Process Analysis, Cork Institute of Technology, Cork, Ireland, and Tyndall National Institute, Cork, Ireland.
*Corresponding authors. E-mails: kostsakmakidis@gmail.com, rboyd@uottawa.ca

A century-old tenet in physics and engineering asserts that any type of system, having bandwidth $\Delta\omega$, can interact with a wave over only a constrained time period Δt inversely proportional to the bandwidth ($\Delta t \cdot \Delta\omega \sim 2\pi$). This law severely limits the generic capabilities of all types of resonant and waveguiding systems in photonics, cavity quantum electrodynamics and optomechanics, acoustics, continuum mechanics, atomic and optical physics, but is thought to be completely fundamental, arising from basic Fourier reciprocity. We propose that this 'fundamental' limit can be overcome in systems where Lorentz reciprocity is broken. As a system becomes more asymmetric in its transport properties the degree to which the limit can be surpassed becomes greater. By way of example, we theoretically demonstrate how in an astutely designed magnetized semiconductor heterostructure the above limit can be exceeded by orders of magnitude using realistic material parameters. Our findings revise prevailing paradigms for linear, time-invariant resonant systems, challenging the doctrine that high-quality resonances must invariably be narrowband, and providing the possibility of developing devices with unprecedently high time-bandwidth performance.

More than 100 years ago, K. S. Johnson introduced the concept of the now-ubiquitous *Q*-factor to characterize the sharpness of a resonance (*1*, *2*). In that work, a practical way to characterize the quality of a resonant system was introduced by defining a unitless number, $Q = \omega_0/\Gamma$, where ω_0 is the system's resonance frequency and Γ the decay rate of the wave energy (*1*, *2*). Ever since then, it has been understood that the higher the *Q*-factor of a resonant system, the narrower becomes its bandwidth – higher *Q*s lead to sharper resonances (*1*).

This notion, that high-quality (high-*Q*) resonances must invariably be narrowband, has not been challenged since Johnson's original work, and pervades an extremely broad range of resonant and waveguiding systems in physics and engineering (Fig. 1). Its justification arises from basic Fourier-reciprocity considerations (*3*-*5*): Inside any linear, passive (lossy and time-invariant) resonant system, e.g., in a cavity micro-/nano-resonator, the excited wave amplitude $\alpha(t)$ will decay as $\alpha(t) \propto \cos(\omega_0 t) \times e^{-(1/2)\Gamma t}$, where the total decay rate Γ can be due to nonradiative (inelastic or dephasing) and/or radiative processes (coupling to the continuum of the surrounding medium). Hence, in the resonance

approximation and in the usual underdamped regime ($\Gamma/2 << \omega_0$) (*3*, *4*), the intensity *I* in the frequency domain will be given by

$$I(\omega) \propto |\alpha(\omega)|^2 \propto \frac{\left(\frac{\Gamma}{2}\right)^2}{(\omega-\omega_0)^2+\left(\frac{\Gamma}{2}\right)^2}, \tag{1}$$

from which it is immediately seen that the bandwidth $\Delta\omega$ around ω_0 is: $\Delta\omega = (\omega_0 + \Gamma/2) - (\omega_0 - \Gamma/2) = \Gamma$. Thus, by definition, the bandwidth of the resonant system is the loss rate, Γ. Any attempt to reduce the overall losses and hence store the wave for an increased time $\Delta\tau$ will automatically decrease the bandwidth $\Delta\omega$ – a limitation that arises from simple time-harmonic considerations.

We show that this 'fundamental' time-bandwidth limit characterizing resonant devices can be overcome by breaking Lorentz reciprocity, i.e. by conceiving (asymmetric) systems whose response changes when the source and the receiver are interchanged:

$$\iiint_V \mathbf{J}_1\mathbf{E}_2 dV \neq \iiint_V \mathbf{J}_2\mathbf{E}_1 dV, \tag{2}$$

where $\mathbf{J}_1$ and $\mathbf{J}_2$ are two sources within a volume *V* generating, respectively, the fields $\mathbf{E}_1$ and $\mathbf{E}_2$. Specifically, we shall introduce and analyze a realistic system that exceeds the time-bandwidth limit anticipated by the system's *Q*-factor by orders of magnitude.

We note that the time-bandwidth (T-B) limitation is a completely general phenomenon, characterizing the storage capacity of all linear, time-invariant resonant and waveguiding devices, from photonics to acoustics, cavity quantum electrodynamics and opto-mechanics, atomic and molecular physics, as well as mechanical and structural systems (Fig. 1). It should not be confused with the mathematical time-bandwidth limit, $\sigma_t^2\sigma_\Omega^2 \geq 1/4$, σ_t^2 being the time variance of a signal $x(t) \in L_2(\Re)$ and σ_Ω^2 its frequency variance, i.e., with the uncertainty principle characterizing Fourier-integral pairs in signal analysis and communications (*6*) and which, among others, only has a lower bound. Although both limits often bear the same name, the T-B limit in physics and engineering characterizes the storage capacity of the devices themselves – not the mathematical Fourier properties of the respective signals. In addition to resonant physical devices outlined above, the physical T-B limit studied herein also arises in guiding structures, such as slow-light waveguides or bulk media (e.g., electromagnetically induced transparency in ultracold atomic gases) (*7-12*). Here, a number of works have shown that any such passive structure can support slow waves over a finite bandwidth $\Delta\omega$ inversely proportional to the group index n_g. Hence, a structure of fixed length *L* cannot delay a wavepacket of bandwidth larger than $\Delta\omega$ by more than a time $\Delta\tau \sim n_g L/c$, where *c* is the speed of light in vacuum. In other words, the 'delay-bandwidth product', $\Delta\tau\cdot\Delta\omega$, characterizing a linear, time-invariant slow-wave structure has an upper limit, *C* (*13-15*). This threshold is quite stringent: Depending on the specifics of the particular slow-wave structure, it can vary between $C \sim$10-100, to within an order of magnitude (*7-10*, *13-15*) and cannot be broken by means of a nonlinear or gain mechanism, such as stimulated Raman or stimulated Brillouin scattering, because such fundamental effects as gain saturation, group-velocity and attenuation dispersions make, in fact, $\Delta\tau$ inversely proportional to a power of $\Delta\omega$ – e.g., $\Delta\tau \sim \Delta\omega^{-\alpha}$, α = 2, 3 (*7*, *9*, *14*); an even stricter limitation. A further adverse consequence of the time-bandwidth limit in physics and engineering is that it constrains the response time of the above devices, since the higher the *Q*-factor of a system (i.e., the narrower the bandwidth) the longer it takes to respond to an external signal. But a high *Q*-factor is a prerequisite for high sensitivity (*16*). Thus, short response times and high sensitivity tend to counteract each other and a compromise has to be found between the two. A well-known

manifestation of this limitation concerns microfabricated quartz tuning forks – currently, the most successful and widespread method for shear-force detection. With a Q-factor at ambient conditions of the order of 10^3-10^4 – necessary for probing interaction forces smaller than ~200 pN –, the response time of a tuning fork, $\tau = 2\sqrt{3}Q/\omega_0$, is limited to be larger than ~300 ms (*16*), i.e., the scanning speeds are slow.

To overcome the time-bandwidth limit by breaking Lorentz reciprocity, consider a wave s_+ impinging (either from a surrounding uniform medium or from a guiding structure) on a reciprocal system, and exciting a mode of amplitude α inside it (Fig. 2A). The key idea is to realize that while the basic Fourier-transform reciprocal relations do, in general, remain valid, they can be applied separately at the input and output ports of a system if it is asymmetric (nonreciprocal) in its transport properties, i.e. if Lorentz reciprocity is broken. The equation describing the time-evolution of $\alpha(t)$ is (*17*)

$$\frac{d\alpha}{dt} = j\omega_0\alpha - \left(\frac{1}{\tau_0} + \frac{1}{\tau_{out}}\right)\alpha + \rho_{in}s_+, \tag{3}$$

where ω_0 is the resonance frequency, $1/\tau_0$ and $1/\tau_{out}$ are the internal (owing, e.g., to dissipative losses) and out-coupling (owing, e.g., to radiative loss to the surrounding medium) decay rates, respectively, and ρ_{in} is the rate of in-coupling of energy from the s_+ wave to the resonant system. Here, following the standard convention of temporal coupled-mode theory, we assume that $|s_+|^2$ is normalized to the incident power, whereas $|\alpha|^2$ is normalized to the incident energy (i.e., the units of $|s_+|$ are $\sqrt{2W/s}$) (*17*). The rate of in-coupling of energy into the resonant system, ρ_{in}, is proportional to the bandwidth $\Delta\omega$ of the system ($\pi\rho_{in} \leftrightarrow \Delta\omega$) (*17, 18*) [see also Supplementary Materials, SM (*19*)], while the lifetime $\Delta\tau$ of the excited mode is, as shown from Eq. (3), $\Delta\tau = 1/(1/\tau_0 + 1/\tau_{out}) \approx \tau_{out}$ – since we normally operate in the overcoupled (underdamped) regime where the rate of energy escape from (and energy coupled into) the excited resonant system is greater than the rate of internal dissipation, $2/\tau_{out} >> 2/\tau_0$. The key point is that, because of time-reversal symmetry, it can be shown rigorously that the in-coupling rate, ρ_{in}, is always tied to the out-coupling rate, ρ_{out}, via the exact relation (in units of $|\alpha|$) (*17*):

$$|\rho_{in}| = \frac{2}{\tau_{out}}. \tag{4}$$

Thus, the product between the system's bandwidth and the wave-system interaction time (lifetime) $\Delta\tau$ is always, for reciprocal systems, of the order of: $\Delta\omega\Delta\tau \leftrightarrow \pi|\rho_{in}|\tau_{out} \sim 2\pi$, i.e. we recover the aforesaid physical time-bandwidth limitation, in which $\Delta\omega$ and $\Delta\tau$ characterizing a resonant or guiding device are reciprocally related. However, if Lorentz reciprocity is by some means broken in this passive, linear and time-invariant resonant system, $|\rho_{in}|$ and τ_{out} can become completely decoupled, in which case the product $\Delta\omega\Delta\tau$ (or, equivalently, $|\rho_{in}|\tau_{out}$) can be engineered at will and take on arbitrarily large values – i.e., in such a case we can exceed the conventional time-bandwidth limit by an arbitrarily large factor.

Consider a heterostructure made of a dielectric layer (silicon, Si) bounded asymmetrically by a gyroelectric semiconductor (indium antimonide, InSb) on the bottom and a metal layer (silver, Ag) on the top (Fig. 2B). Lorentz reciprocity in this linear, passive and time-invariant system can be broken by applying a static magnetic field B_0 in the -y direction (*20-22*), causing a precession of the electron magnetic dipole moments in the semiconductor with a frequency $\omega_c = eB_0/m^*$ (e and m^* being the charge and effective mass of the electrons, respectively). A small AC magnetic field propagating along the heterostructure also causes a precession of the semiconductor electrons' dipole moments around

the B_0 (-y) axis at the frequency of the AC field. The interaction of the AC field with the semiconductor is, thus, overall, captured by the following asymmetric permittivity tensor (*23*):

$$\varepsilon = \varepsilon_0 \varepsilon_\infty \begin{bmatrix} \varepsilon_1(B_0) & 0 & i\varepsilon_2(B_0) \\ 0 & \varepsilon_3 & 0 \\ -i\varepsilon_2(B_0) & 0 & \varepsilon_1(B_0) \end{bmatrix}, \tag{5}$$

where $\varepsilon_1 = 1 - (\omega + iv)\omega_p^2/\{\omega[(\omega + iv)^2 - \omega_c^2]\}$, $\varepsilon_2 = \omega_c\omega_p^2/\{\omega[(\omega + iv)^2 - \omega_c^2]\}$, $\varepsilon_3 = 1 - \omega_p^2/[\omega(\omega + iv)]$, with the plasma frequency of InSb taken to be $\omega_p = 4\pi \times 10^{12}$ rad/s ($f_p = 1/T_p = 2$ THz), $\varepsilon_\infty = 15.6$, $\omega_c = 0.2\omega_p$, and $B_0 = 0.2$ T. For the other two layers, we take $\varepsilon_{Si} = 11.68$, and $\varepsilon_{Ag} = 1 - \omega_{pe}^2/[\omega(\omega + i\omega_\tau)]$, with $\omega_{pe} = 1.367 \times 10^{16}$ rad/s and $\omega_\tau = 2.733 \times 10^{13}$ rad/s (*20, 21, 23*). Because of the application of the external magnetic bias, the heterostructure supports one-way edge (magnetoplasmon) modes, robust against surface imperfections and roughness, whose dispersion relation is governed by (*20*, *21*, *23*):

$$\tanh(\alpha_d d) = -\frac{\alpha_s + \frac{\varepsilon_2}{\varepsilon_1}k + \frac{\varepsilon_V \alpha_m}{\varepsilon_m}}{\left(\alpha_s + \frac{\varepsilon_2}{\varepsilon_1}k\right)\frac{\varepsilon_r \alpha_m}{\varepsilon_m \alpha_r} + \frac{\varepsilon_V \alpha_d}{\varepsilon_r}}, \tag{6}$$

where $\alpha_d = \sqrt{k^2 - \varepsilon_r k_0^2}$, $k_0 = \omega/c$ being the vacuum wavenumber, $\varepsilon_r = \varepsilon_{Si}$ and $d = 0.08\lambda_p$ ($\lambda_p = 2\pi c/\omega_p$) are the relative permittivity and thickness of the Si layer, respectively, $\alpha_s = \sqrt{k^2 - \varepsilon_V k_0^2}$, $\varepsilon_V = \varepsilon_\infty(\varepsilon_1 - \varepsilon_2^2/\varepsilon_1)$ being the Voigt permittivity, and $\alpha_m = \sqrt{k^2 - \varepsilon_m k_0^2}$, with ε_m being the relative permittivity of Ag.

Upon solving Eq. (6), we plot in Fig. 2C the band structure of this type of surface states, showing clearly that the band diagram is asymmetric with respect to the wavevector-k axis, giving rise to a frequency region where no backward-propagating ($k < 0$) states exist (breaking of Lorentz reciprocity). For a carefully designed structure, that region can be made to be below the continuous band(s) of the bulk modes in the semiconductor and above the band associated with surface states at the semiconductor-metal interface. Thus, in that frequency region, complete unidirectional propagation (CUP) is rigorously attained: An excited edge state can propagate strictly only in the forward (positive z, k) direction, and cannot be back-reflected or couple to bulk modes in the semiconductor, nor to semiconductor-metal surface states. The two frequencies, ω_{CUP}^- and ω_{CUP}^+, bounding the CUP region (see Fig. 2C) can be identified analytically from Eq. (6) by letting $|k| \to \infty$ [see SM (*19*)]:

$$\omega_{CUP}^{\pm} = \frac{1}{2}\left(\sqrt{\omega_c^2 + 4\omega_p^2 \frac{\varepsilon_\infty}{\varepsilon_\infty + \varepsilon_r}} \pm \omega_c\right), \tag{7}$$

from where we see that the bandwidth of the CUP region is simply: $BW_{CUP} = \omega_c$ (= eB_0/m^*).

Figure 3A illustrates successive snapshots from full-wave simulations of the propagation of a pulse, whose bandwidth is within the CUP region, along the heterostructure of Fig. 2B. The structure is terminated in the z direction by the Ag cladding (which also covers the end of the heterostructure), creating an impenetrable barrier for the pulse along z. Since, in that frequency region, there are no surface modes allowed at the Ag/InSb interface, and the pulse cannot scatter to bulk modes inside InSb nor to backward modes in the -z direction (see Fig. 2C), the pulse eventually localizes near the Si/Ag interface, where it decays with time until it is completely absorbed (right panel of Fig. 3A). As seen from Fig. 3A, initially, the pulse broadens (because of dispersion) to a longitudinal length, at $t = 15$ ps (= $30T_p$),

of $d_i^{\ell} \cong 215.5$ μm [and a transverse size of $d_i^{T} \cong 12.1$ μm; see also SM Figs. S1A-B (*19*)] but when it reaches the rightmost end it gives rise to a strongly localized plasmonic resonance: at t = 50 ps (= $100T_p$) it is spatially compressed to a deep-subwavelength spot of $d_f^{\ell} \cong 0.165$ μm (and $d_f^{T} \cong 0.02$ μm), i.e. it is spatially squeezed by a factor of ~0.79×10^6 in two dimensions, while its peak intensity is enhanced by a factor of ~10^3 [see also SM Figs. S1D-E (*19*)]. The localized field, thus, behaves exactly as if it were confined inside a subwavelength, 'zero-dimensional' (*24*) cavity resonator perfectly matched to the incident-wave medium: It is confined in a specified region of space, where it was in-coupled without reflections, decaying with time inside (but not propagating within nor escaping from) this region, and with the field amplitude being dramatically enhanced inside this zero-dimensional cavity. Figure 3B further shows that the so-trapped field can be released on-demand by reversing the direction of the external magnetic bias B_0 (B_0 = 0.2 T → B_0 = –0.2 T) at any point while the field is localized. A somewhat reminiscent light-trapping, storage and releasing scheme also exists, e.g., for ultraslow and stored light in atomic EIT (*8*, *11*, *12*) but with the fundamental difference that therein the bandwidth is narrow (*25*) and/or the attained storage times are inversely proportional to the bandwidth (or to a power of it) (*7*, *9*, *13-15*). Supplementary Materials Fig. S2 (*19*) shows how in this linear, time-invariant system the whole broad spectrum of the pulse is progressively stored in its trapping region.

Because of the above Lorentz-reciprocity-breaking characteristics, the rates of in-coupling (ρ_{in}) and out-coupling (ρ_{out}) of energy in this open cavity are not equal: while ρ_{in} is proportional to the system's in-coupling bandwidth ($\rho_{\text{in}} \propto \Delta\omega_{\text{in}}$), the out-coupling rate tends to zero ($\rho_{\text{out}} = 1/\tau_{\text{out}} \rightarrow 0$), since the lightwave cannot radiatively escape from the region it is confined in. Thus, based on our previous analysis, we expect that in this system the interaction time $\Delta\tau = 1/(1/\tau_0 + 1/\tau_{\text{out}}) \approx \tau_0$ and the resonant bandwidth $\Delta\omega$ should be completely decoupled – not inversely proportional as in all conventional (reciprocal) resonant and waveguiding systems. In other words, we expect that our system can be extremely broadband even in the limit of ultrahigh Q-factors where the total losses may tend to zero and the storage times to infinity ($\Delta\tau \rightarrow \infty$).

To demonstrate that $\Delta\tau$ and $\Delta\omega$ are independent of one another, Fig. 4 summarizes the results of successive full-wave simulations for the cases where (i) the loss rate ν is progressively increased but B_0 remains constant, and (ii) B_0 progressively increases but ν remains constant. We see from Figs. 4A-B that while ν is increased, the total optical losses of the system progressively increase, too, as expected, but the bandwidth of the effective cavity remains constant in all cases, $\Delta\omega \approx 2.5$ THz – unaffected by the gradually increased loss rate. Even in the case where an extremely low-loss InSb film ($\nu/\omega_p = 10^{-4}$) with realistic material parameters is used [e.g., electron density $N_e = 1.1\times10^{16}$ cm^{-3}; see (*26*) and SM (*19*)], we find that whereas the energy decay rate Γ is ~10^9 s^{-1} and therefore the bandwidth $\Delta\omega$ should conventionally be anticipated to be small, ~10^{-3} THz ($\Delta\omega = \Gamma$, see discussion immediately after Eq. (1)), the actual bandwidth of the non-reciprocal zero-dimensional cavity at the rigthmost end of our structure is still large and ~2.5 THz – more than 3 orders of magnitude above the fundamental time-bandwidth limit of reciprocal (linear and passive) systems. Furthermore, we find that the pulse is seamlessly in-coupled to the localization point (whereas for any reciprocal, lossless resonant system the in-coupling time would have tended to infinity for progressively smaller losses), where it is rigorously confined (Fig. 3A and leftmost parts of Figs. 4A, 4B). Thus, the performance of this system, both in terms of bandwidth and response time, exceeds that of any standard reciprocal system (*4*, *5*, *16-18*, *23*, *24*) by orders of magnitude.

For case (ii), where the external static magnetic field B_0 progressively increases, Figs. 4C-D show that the bandwidth of the zero-dimensional cavity increases accordingly (by a factor of 100%), as expected from Eq. (7), but the optical losses (and, hence, the storage times) remain approximately constant, increased only by a factor of ~5% – unaffected by the bandwidth increase. The small increase in the total optical losses that we observed in our simulations for this latter case is because the slope of the band

(i.e., the pulse's group velocity) reduces with increasing B_0, leading to higher overall optical losses (*27*). We see from Figs. 4C-D that, in this case too, the nonreciprocal cavity is above the fundamental time-bandwidth limit of conventional (reciprocal) resonant systems by more than two orders of magnitude. The results of Fig. 4, therefore, convincingly show that in this system the interaction time (lifetime) $\Delta\tau$ and the bandwidth $\Delta\omega$ are independent/decoupled of one another, owing to the breaking of Lorentz reciprocity ($\rho_{in} >> \rho_{out}$), giving rise to an, in principle, unlimited time-bandwidth performance – i.e., to breaking of the *Q*-factor limit in the sense that $\Delta\tau$ and $\Delta\omega$ are not inversely proportional to one another anymore [although Fourier uncertainty (*6*) is still obeyed when considered separately at the input and output ports, as shown in Fig. 2A and discussed above].

Finally, we note that in existing, reciprocal ultraslow- and stored-light configurations (e.g., those exploiting dark states in electromagnetically induced transparency, EIT, or in coherent populations trapping) the storage time is fundamentally inversely proportional to the system's bandwidth or to a power of it (*7-15*). In contrast, in the present nonreciprocal scheme the storage time is solely determined by the loss rate (which, as we saw from Fig. 4, is decoupled from the bandwidth) and/or the time until which we switch off the external magnetic field, releasing the localized pulse (Fig. 3B). Since both of these parameters (loss rate and duration of B_0 being "on") are, here, completely independent of the system's bandwidth, the attained delay-bandwidth products can now, in principle, become arbitrarily large. For instance, Fig. 3B demonstrates storage times of up to ~400 T_p for a pulse of bandwidth 0.2 THz, whereas conventionally, for reciprocal guiding structures, the anticipated maximum delay and storage times would be (*7-15*) Δt_{max} ~(bandwidth)$^{-1}$, or less, i.e., Δt_{max} ~5 ps = 10 T_p. Thus, our non-reciprocal device is above the conventioanl delay-time/bandwidth limit of state-of-the-art slow-light systems by more than a factor of 40.

The consequences of our findings carry over to all resonant and waveguiding systems in physics and engineering where the above time-bandwidth limit appears in disguise, including subdiffraction imaging systems (where there is always a tradeoff between spatial and temporal resolution) (*28*) and broadband invisibility cloak devices (where there is a tradeoff between scattering reduction and broadband operation) (*29*, *30*). On a more fundamental level, our results reveal that the time-bandwidth and *Q*-factor limits characterizing the storage capacity of (passive, linear) guiding and resonant systems in physics and engineering is not as 'fundamental' as has conventionally been thought and can be broken to an arbitrarily large degree, so long as Lorentz reciprocity is broken in those systems. To this end, further means of breaking unidirectionality (*22*), such as parity-time-symmetry media (*31*) or topological insulators (*32-34*) might also of interest. We believe that it is now possible to design ultrahigh-*Q* resonant systems in atomic, optical and condensed matter physics, as well as in mechanical and electrical engineering, with unprecedentedly high bandwidths and ultrafast response times, as well as ultraslow- and stopped-light systems with unusually high delay-bandwidth products, for a wide range of applications in those fields (*3*, *8-10*, *16-18*, *23*, *24*).

References:

[1] E. I. Green, "The story of *Q*," *American Scientist* **43**, 584-594 (1955). (available online at: http://www.collinsaudio.com/Prosound_Workshop/The_story_of_Q.pdf)

[2] K. S. Johnson, *Transmission Circuits for Telephonic Communication* (D. Van Nostrand, 1925, and Western Electric, 1924).

[3] A. E. Siegman, *Lasers* (Univ. Science Books, 1986), pp. 105–108.

[4] K. J. Vahala, "Optical microcavities," *Nature* **424**, 839-846 (2003).

[5] W. Ketterle, MIT 8.421 Atomic and Optical Physics I, Spring 2014 (MIT OpenCourseWare, 2014). (available online at: http://ocw.mit.edu/8-421S14), min.: 1:09:00.

[6] A. Papoulis, *Signal Analysis*, sec. 8.2 (McGraw-Hill, New York, 1977).

[7] R. W. Boyd, D. J. Gauthier, A. L. Gaeta, and A. E. Willner, "Maximum time delay achievable on propagation through a slow-light medium," *Phys. Rev. A* **71**, 023801 (2005).
[8] P. W. Milonni, *Fast Light, Slow Light, and Left-Handed Light* (Institute of Physics, 2005).
[9] J. B. Khurgin and R. S. Tucker (eds.), *Slow Light: Science and Applications* (Taylor & Francis, 2009).
[10] R. W. Boyd, "Controlling the velocity of light pulses," *Science* **326**, 1074-1077 (2009).
[11] L. V. Hau, S. E. Harris, Z. Dutton, and C. H. Behroozi, "Light speed reduction to 17 metres per second in an ultracold atomic gas," *Nature* **397**, 594–598 (1999).
[12] M. D. Lukin and A. Imamoğlu, "Controlling photons using electromagnetically induced transparency," *Nature* **413**, 273–276 (2001).
[13] D. A. B. Miller, "Fundamental limit to linear one-dimensional slow-light structures," *Phys. Rev. Lett*. **99**, 203903 (2007).
[14] J. B. Khurgin, "Slow light in various media: a tutorial," *Adv. Opt. Photon*. **2**, 287-318 (2010).
[15] Q. Xu, P. Dong, and M. Lipson, "Breaking the delay-bandwidth limit in a photonic structure," *Nature Physics* **3**, 406-410 (2007).
[16] L. Novotny and B. Hecht, *Principles of Nano-Optics* (Cambridge Univ. Press, 2012).
[17] H. A. Haus, *Waves and Fields in Optoelectronics* (Prentice-Hall, 1984), ch. 7.
[18] K. Vahala, *Optical Microcavities* (World Scientific, 2005).
[19] See supplementary materials.
[20] J. J. Brion, R. F. Wallis, A. Hartstein, and E. Burstein, "Theory of surface magnetoplasmons in semiconductors," *Phys. Rev. Lett*. **28**, 1455-1458 (1972).
[21] L. Shen, Y. You, Z. Wang, and X. Deng, "Backscattering-immune one-way surface magnetoplasmon at terahertz frequencies," *Opt. Express* **23**, 950-962 (2015).
[22] D. Jalas, *et al*., "What is – and what is not – an optical isolator," *Nature Photon*. **7**, 579-582 (2013).
[23] D. M. Pozar, *Microwave Engineering* (Wiley, 2011).
[24] S. M. Dutra, *Cavity Quantum Electrodynamics: The Strange Theory of Light in a Box* (Wiley, 2005), p. 34.
[25] R. Zhang, S. R. Garner, and L. V. Hau, "Creation of long-term coherent optical memory via controlled nonlinear interactions in Bose-Einstein condensates," *Phys. Rev. Lett*. **103**, 233602 (2009).
[26] J. G. Rivas, C. Janke, P. H. Bolivar, and H. Kurz, "Transmission of THz radiation through InSb gratings of subwavelength apertures," *Opt. Express* **13**, 847-859 (2005).
[27] R. W. Boyd, "Material slow light and structural slow light: similarities and differences for nonlinear optics," *J. Opt. Soc. Am. B* **28**, A38-A44 (2011).
[28] W. H. Wee and J. B. Pendry, "Universal evolution of perfect lenses," *Phys. Rev. Lett*. **106**, 165503 (2011).
[29] U. Leonhardt and T. Tyc, "Broadband invisibility by non-Euclidean cloaking," *Science* **323**, 110-112 (2009).
[30] F. Monticone and A. Alù, "Invisibility exposed: physical bounds on passive cloaking," *Optica* **3**, 718-724 (2016).
[31] C. E. Rüter, *et al*., "Observation of parity-time symmetry in optics," *Nature Physics* **6**, 192-195 (2010).
[32] M. Z. Hasan and C. L. Kane, "*Colloquium*: Topological insulators," *Rev. Mod. Phys*. **82**, 3045 (2010).
[33] M. C. Rechtsman, *et al*., "Photonic Floquet topological insulators," *Nature* **496**, 196-200 (2013).
[34] A. B. Khanikaev, *et al*., "Photonic topological insulators," *Nature Materials* **12**, 233-239 (2013).

ACKNOWLEDGMENTS
The authors gratefully acknowledge the support of the Eugen Lommel fellowship of the Max Planck Institute for the Science of Light (Erlangen) and the Canada Excellence Research Chairs Program.

SUPPLEMENTARY MATERIALS
www.sciencemag.org/content/
Supplementary Materials and Methods
Figs. S1(A)–(E), S2(A) –(C), S3(A), (B)
Table S1

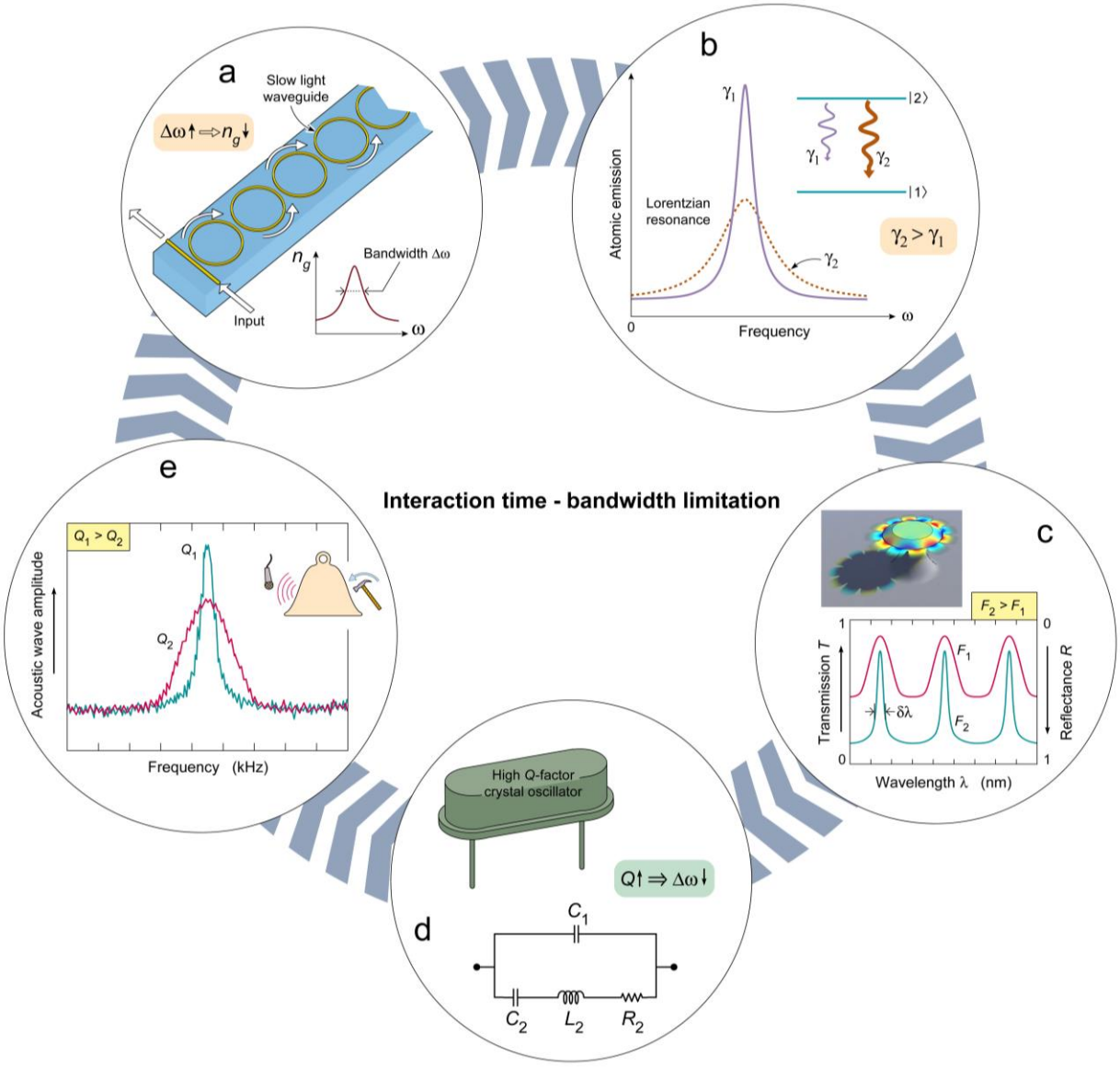

Fig. 1. The 'fundamental' time-bandwidth limit, in various forms, in reciprocal systems in physics and engineering. (**A**) In all types of slow-light waveguides, the attained delays Δt are inversely proportional to the guide's bandwidth, $\Delta\omega$ ($\Delta t \propto \Delta\omega^{-1}$) or, even more severely, to a power of it (e.g., $\Delta t \propto \Delta\omega^{-\alpha}$, α = 2 or 3) (*7-15*). (**B**) In atomic and molecular physics, the linewidth γ of an atomic transition is inversely proprotional to the decay rate arising from dephasing and inelastic or spontaneous-emission processes (*3*). Likewise, the time required to perform the transformation $|\Psi_i\rangle \rightarrow |\Psi_f\rangle = e^{-iHt}|\Psi_i\rangle$, where $|\Psi_i\rangle$ and $|\Psi_f\rangle$ are two orthogonal states, and H is the (time-independent) Hamiltonian, is $\tau_{tr} \sim |(E_f - E_i)/\hbar|^{-1}$, where E_f and E_i are the corresponding eigenvalues of H (*24*). (**C**) In all types of (dielectric or plasmonic) cavity resonators, higher finesses F result in narrower resonance bandwidths (*3-5*, *16-18*). (**D**) In crystal (quartz) oscillators, piezoelectic, micro-/nano-mechanical or elastic systems and energy-harvesting devices, the response times are directly proportional to the system's Q-factor, $\tau_{rsp} \propto Q$. Higher Q-factors lead to enhanced sensitivities but also to larger response times (*16*). (**E**) In acoustic devices and systems, such as in ultrasound, elastic-wave, or wave-modulation spectroscopies, increased quality factors give rise to narrower spectral responses.

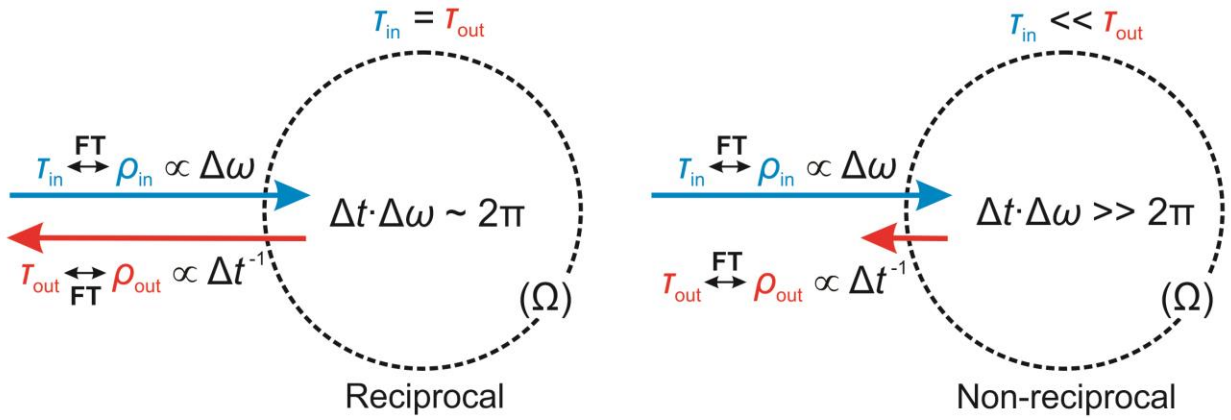
$T_{in} = T_{out}$
$T_{in} \overset{FT}{\leftrightarrow} \rho_{in} \propto \Delta\omega$
$\Delta t \cdot \Delta\omega \sim 2\pi$
$T_{out} \overset{FT}{\leftrightarrow} \rho_{out} \propto \Delta t^{-1}$
(Ω)
Reciprocal
$T_{in} << T_{out}$
$T_{in} \overset{FT}{\leftrightarrow} \rho_{in} \propto \Delta\omega$
$\Delta t \cdot \Delta\omega >> 2\pi$
$T_{out} \overset{FT}{\leftrightarrow} \rho_{out} \propto \Delta t^{-1}$
(Ω)
Non-reciprocal

(A)

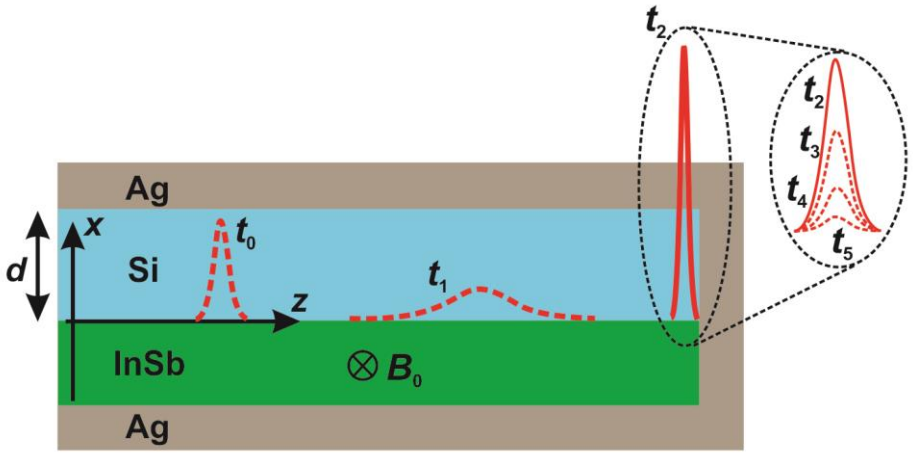
Ag
Si
InSb
Ag
d
x
z
t_0
t_1
t_2
t_3
t_4
t_5
$\otimes B_0$

(B)

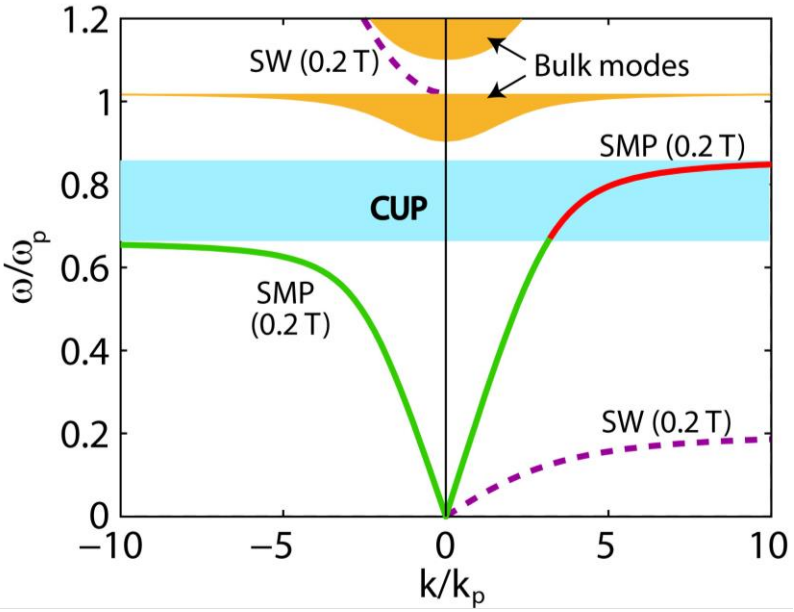
SW (0.2 T)
Bulk modes
SMP (0.2 T)
CUP
SMP
(0.2 T)
SW (0.2 T)
ω/ω_p
k/k_p
1.2
1
0.8
0.6
0.4
0.2
0
−10
−5
0
5
10

(C)

Fig. 2. Concept and structure for overcoming the time-banwidth limit. (**A**) In a reciprocal system (left panel), the rate ρ_{in} with which energy enters the system is equal to the rate ρ_{out} with which energy exits the system. This leads to the interaction time being inversely proportional to the system's bandwidth, $\Delta t \propto \Delta\omega^{-1}$. By contrast, in a non-reciprocal system (right panel) the in-coupling time, τ_{in}, can be much shorter than the out-coupling time, $\tau_{in} << \tau_{out}$ (or, equivalently, $\rho_{in} >> \rho_{out}$), leading to an interaction time Δt that can be completely decoupled from the bandwidth $\Delta\omega$. Consequently, the product $\Delta t \cdot \Delta\omega$ can now take on arbitrarily large values – much larger than the standard '2π' limit. Note that in both cases the Fourier-transform reciprocity, relating τ_{in} (τ_{out}) to ρ_{in} (ρ_{out}) and to $\Delta\omega$ (Δt^{-1}), is always valid – but is applied *separately* to the input and the output of the system. (**B**) Schematic illustration of the non-reciprocal configuration used for breaking the time-bandwidth limit. It consists of a Si layer sitting on top of a gyroelectric semiconductor, InSb. The two layers are bounded by Ag on three sides. The external, static magnetic field B_0 is applied in the -*y* direction. A pulsed magnetic-current source excites a surface magnetoplasmon, which propagates unidirectionally, without back-scattering or back-reflections, from left to right, all the way until the rightmost Si/Ag interface where it is spatially compressed, greatly enhanced in amplitude and robustly localized (cf. Fig. 3A). There are no propagating states allowed in the -*z* direction, nor inside InSb, nor along the InSb/Ag interface (see also (**C**)). Once localized at the rigthmost end, a pulse can only decay with time owing to dissipative losses, exactly as if it were confined inside a passive, 'zero-dimensional' (*23*) cavity resonator (right inset). (**C**) Band diagram of the structure of (**B**) for the case where the external magnetic field is applied in the -*y* direction (B_0 = 0.2 T). Shown are, both for positive and negative longitudinal wavevectors *k*, the dispersion curve of the herein studied surface magnetoplasmons (SMPs), the surface wave at the InSb/Ag interface (SW), and the region of the bulk modes in InSb. The area shaded in pale blue indicates the band region where complete unidirectional propagation (CUP) of the considered surface magnetoplasmon is attained. The part of the SMP dispersion curve inside that region is indicated with red color.

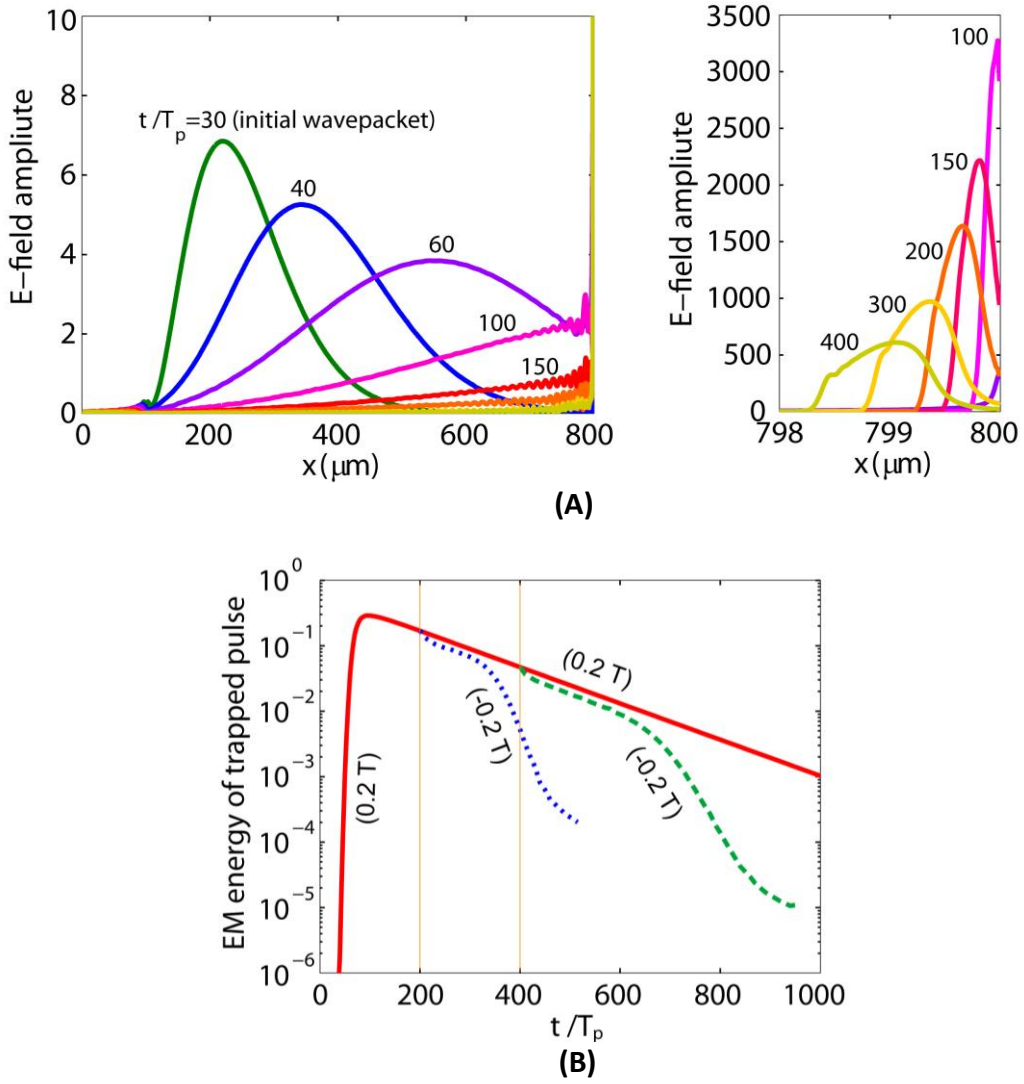

Fig. 3. Open cavity localization and overcoming the 'fundamental' delay-time/bandwidth limit. (**A**) One-dimensional snapshots of the propagation of a pulse of central frequency 1.5 THz and bandwidth 0.2 THz, exciting a one-way surface magnetoplasmon in the heterostructure of Fig. 2B, at successive time instants. The right panel shows zoomed-in snapshots around the localization region at the rightmost end of the heterostructure of Fig. 2B. Note the change in the scale of the vertical axis and the dramatic ensuing field enhancement upon entering that zero-dimensional open-cavity region. (**B**) Electromagnetic energy as a function of time in an imaginary 'box' surrounding the pulse's localization region. When the external static magnetic field B_0 = 0.2 T is constantly in the -*y* direction, the energy of the localized pulse inside the box simply decays with time (red curve) owing to dissipative losses, as expected (and as shown in **A**). By contrast, when the direction of the B_0 field is suddenly reversed (B_0 = –0.2 T), the pulse may now escape in the backward (-*z*) direction (cf. Fig. 2C), as a result of which the wave energy inside the box rapidly diminishes. Two examples of this are shown here, one at t = 200 T_p (blue dotted) and another at t = 400 T_p (green dotted), demonstrating storage times of up to ~400 T_p.

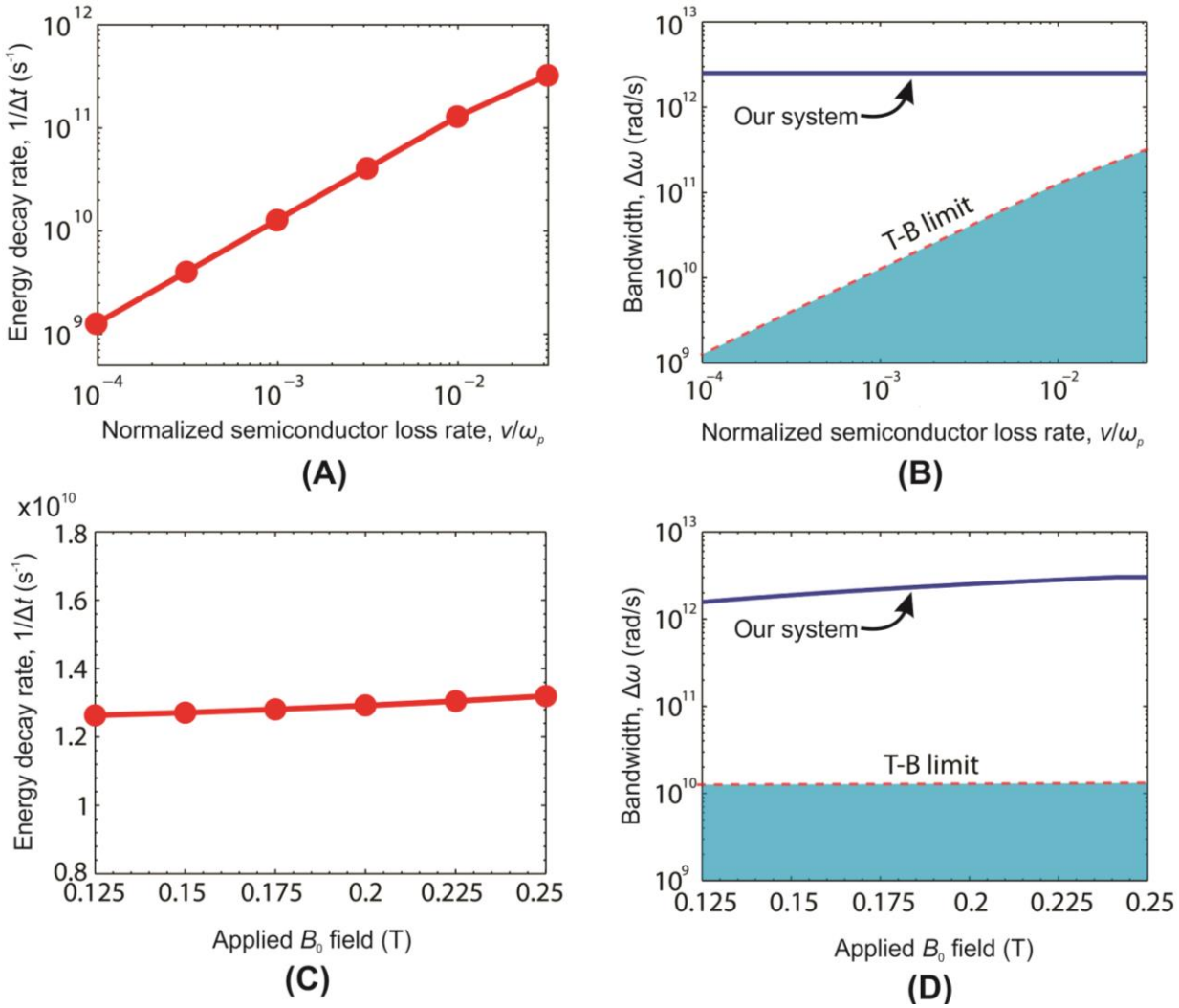

Fig. 4. Decoupling of interaction time and bandwidth, and overcoming the Fourier-reciprocity ($\Delta\omega \sim \Delta t^{-1}$) limit. (**A**), (**B**) For increasing scattering losses, ν, in the semiconductor, the decay rate of the localized pulse's energy progressively increases (**A**), signifying reduced interaction (storage) times, as expected, whereas in all cases the bandwidth $\Delta\omega$ of the one-way effective cavity remains constant (**B**) (blue line). In, both, (**B**) and (**D**) the dashed red lines are, respectively, the solid red lines shown in (**A**) and (**C**). The energy decay rate sets the fundamental bandwidth limit ($\Delta\omega = \Gamma \sim \Delta t^{-1}$, 'T-B limit') characterizing conventional, reciprocal systems – and which is here broken by more than three orders of magnitude, as shown in (**B**). On the other hand, for increasing values of the static magnetic bias B_0, the energy decay rate remains approximately constant (**C**) whereas the bandwidth of the zero-dimensional open cavity progressively increases (**D**) (blue line) – see also SM Fig. S3(B) for further clarity (*19*). Note from (**D**) that, in this case, the bandwidth of the zero-dimensional cavity is more than two orders of magnitude above the fundamental time-bandwidth limit of reciprocal resonant devices – i.e., larger than the energy decay rate by more than two orders of magnitude. All the results shown here have been obtained from full-wave and analytic calculations, as detailed in SM (*19*).